PTEP

Prog. Theor. Exp. Phys. **2024** 103C01 (16 pages)
DOI: 10.1093/ptep/ptae146

Comprehensive Analysis of Impurity Detection in Linear Alkyl Benzene–Based Liquid Scintillators Using Infrared Spectroscopy for Enhanced Neutrino Detection

Ji Young Choi[1], Kyung Kwang Joo[1,*], Jubin Park[2,*], and Myung-Ki Cheoun[2,*]

[1]*Center for Precision Neutrino Research (CPNR), Department of Physics, Chonnam National University, Yongbong-ro 77, Puk-gu, Gwangju 61186, Korea*
[2]*Origin of Matter and Evolution of Galaxy (OMEG), Department of Physics, Institute, Soongsil University, Sangdo-ro 369, Dongjak-gu, Seoul, 06978, Korea*
*Email: kkjoo@chonnam.ac.kr (K.K.J.), honolov@ssu.ac.kr (J.P.), cheoun@ssu.ac.kr (M.-K.C.)

Received July 2, 2024; Revised September 4, 2024; Accepted September 26, 2024; Published September 27, 2024

We present a comprehensive analysis of infrared (IR) spectra for linear alkyl benzene (LAB)-based scintillation solutions, focusing on the detection and identification of impurities. Previous research primarily utilized ultraviolet-visible spectroscopy to investigate electronic structures and transitions, whereas our approach emphasizes vibrational transitions and IR spectral characteristics. We specifically examined the presence of common impurities, such as acetone, water, and three impurity compounds (IMP1, IMP2, and IMP3) identified by the JUNO Collaboration. Acetone, a common contaminant from cleaning procedures, was detected by its characteristic absorption peaks at 1200, 1360, and 1700 cm^{-1}. Water, an inevitable by-product of Gd-loaded LAB using a neutralization reaction process, was identified through distinct O-H stretching and H-O-H bending vibrations at 3200–3600 cm^{-1} and 1600 cm^{-1}, respectively. The IR spectra of IMP1, IMP2, and IMP3 were theoretically calculated, revealing unique absorption bands for key functional groups, including carbonyl (C=O), amide (C-N), sulfoxide (S=O), aryl chloride (Ar-Cl), azo (N=N), and ether (C-O-C) groups. The findings confirm the absence of these impurities in the LAB (+ 2,5-Diphenyloxazole [PPO] + 1,4-Bis(2-methylstyryl)benzene [bis-MSB]) sample, ensuring the high performance and accuracy of neutrino detectors. This study demonstrates the effectiveness of IR spectroscopy as a powerful analytical tool for quality assurance in liquid scintillation solutions, providing a robust framework for enhancing the reliability and precision of neutrino detection experiments.

Subject Index C44, C50, H20

1. Introduction

In the RENO [1], Daya Bay [2], SNO^+ [3,4], Double CHOOZ [5], JUNO [6], $JSNS^2$ [7,8], and some future neutrino experiments, linear alkyl benzene (LAB, $C_6H_5 - C_nH_{2n+1}$, $n = 10 \sim 13$) has been proposed for the solvent in liquid scintillators (LSs) [9]. LAB, mass-produced as a precursor for sanitary detergents, is a derivative with an alkyl chain attached to a phenyl group and contains complex chemical impurities at levels ranging from approximately 0.5% to 3%. Impurities generated from raw or fine chemical processes significantly influence the optical properties of LAB-based scintillation solutions. This is because such impurities affect the electronic structure and electronic transitions of LAB, which is reflected in the Ultraviolet/Visible (UV/VIS)

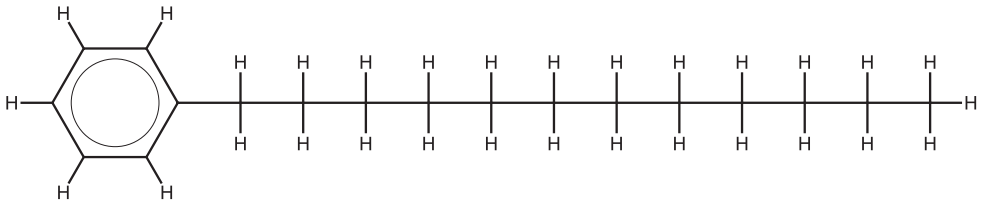

Fig. 1. Molecular structure of dodecylbenzene, a representative compound of LAB. Dodecylbenzene consists of a benzene ring attached to a linear dodecyl (12-carbon) alkyl chain. The benzene ring is an aromatic ring with alternating double bonds, providing a stable and resonant structure. The dodecyl chain is a straight hydrocarbon chain, contributing to the hydrophobic characteristics of LAB. This structure is significant in LAB because the length and configuration of the alkyl chain influence the solubility and interaction with other molecules in scintillation solutions. LAB typically consists of similar compounds with alkyl chains ranging from 10 to 13 carbon atoms.

spectrum. Specifically, LAB exhibits maximum excitation above 350 nm and significantly reduces the light attenuation length in the wavelength of 350–550 nm. This is crucial for photomultiplier tubes (PMTs), which are transparent above 390 nm and sensitive in the 380–500 nm absorption range. To ensure that light resulting from the interaction between neutrinos and Standard Model particles effectively reaches the PMT, it is essential to understand the physical and chemical properties of the solvent and solute, as well as the impurities that affect the attenuation length.

Several studies [10] have focused on the electronic structure and transitions of materials constituting scintillation solutions through the UV/VIS spectrum. However, our study focuses on the vibrational transitions and analyzes the experimental infrared (IR) spectrum results along with theoretical spectrum calculations using the Gaussian16 (G16) software [11]. The IR region is primarily associated with vibrational transitions in molecules, corresponding to wavenumbers from 4000 to 400 cm^{-1}, which cover wavelengths from 2.5 to 25 μm and energies ranging from 0.5 to 0.05 eV. For this purpose, we introduce the solvent LAB and the two solutes as a fluor, 2,5-Diphenyloxazole (PPO, $C_{15}H_{11}NO$) and 1,4-Bis(2-methylstyryl)benzene [bis-MSB, $(CH_3C_6H_4CH = CH)_2C_6H_4$]; we describe their IR measurement experiments and analysis results before discussing the scintillation solutions. LAB, PPO, and bis-MSB incorporate benzene rings as their base structure, which contain unique vibrational modes in the IR region. Additionally, the linear alkyl chains and key functional groups attached to the benzene rings also form specific absorption peaks in the IR spectrum.[1] Therefore, the positions and intensities of these specific absorption peaks provide crucial "fingerprints" for identifying each substance and can assist in predicting how they will react in specific environments. Recently, we discovered that the position of the IR absorption line of LAB is not very sensitive to the length of the alkyl chain, but the absorption intensity changes as the length increases [12]. In particular, by considering dodecylbenzene ($C_6H_5 - C_{12}H_{25} \equiv C_{18}H_{30}$, $n = 12$) as a representative molecule of LAB and comparing LAB IR experimental results, we confirmed that the absorption lines nearly perfectly matched. Figure 1 shows the molecular structure of dodecylbenzene, which comprises a benzene ring attached to a linear dodecyl (12-carbon) alkyl chain. The benzene ring is an aromatic ring with alternating double bonds, providing a stable and resonant structure, while the

[1] In this paper, we primarily discuss transmittance spectra and present the corresponding experimental results. From the perspective of transmittance, a "dip" accurately describes the troughs in the spectra. However, from the absorption perspective, these troughs correspond to peaks. Thus, throughout this paper, the term "peak" is used assuming the absorption perspective.

dodecyl chain is a straight hydrocarbon chain, contributing to the hydrophobic characteristics of LAB. This structure is significant in LAB because the length and configuration of the alkyl chain influence the solubility and interaction with other molecules in scintillation solutions. Next, PPO and bis-MSB were dissolved in LAB to create a scintillation solution. Because the concentrations of these two substances were low in our samples,[2] their unique IR absorption lines were not clearly visible; however, they did affect the intensity of the absorption lines. These results illustrate the impact of interactions among components in mixed solutions on the IR spectrum, providing important information for understanding how the relative concentrations and chemical properties of each component affect the absorption spectrum.

Our main goal is to analyze the IR spectra of the critical impurities in LSs used in neutrino oscillation experiments, such as those performed by the JUNO Collaboration [14]. Although JUNO's research has identified specific impurities affecting the scintillation process, we cannot directly synthesize and introduce these impurities into our solutions owing to experimental limitations and constraints. Instead, our approach focuses on identifying the spectral signatures of these impurities in our scintillator solutions using IR spectroscopy. Accordingly, this work aims to demonstrate the absence of the critical impurities that affect the attenuation length in our own scintillator solutions reported by the JUNO Collaboration. By ensuring that these impurities are not present in our solutions, we can guarantee the purity and suitability of our LS for neutrino detection tasks. Our study not only contributes to the understanding of the effect of impurities on scintillation properties but also demonstrates the effectiveness of IR spectroscopy as one of the powerful analytical tools for quality assurance of LSs used in high-precision neutrino experiments.

To demonstrate practical impurity detection, we introduce two key substances prior to the JUNO Collaboration's impurity analysis and detection: acetone and water. As a first practical example, acetone is widely used in the cleaning and preparation of scientific instruments and optical components due to its rapid evaporation and residue-free properties. However, any residual acetone before complete evaporation can contaminate the sample. By identifying three major acetone absorption peaks corresponding to 1200, 1400, and 1700 cm^{-1} in the LAB solution mixed with PPO, contamination by acetone can be easily detected. As a second practical example, in neutrino oscillation experiments using Gd-loaded LAB, the formation of water during the preparation process is of significant concern. In the synthesis of Gd-carboxylate complexes, neutralization reactions occur, which can be summarized in two steps. The first step involves neutralizing the carboxylic acid (RCOOH) with ammonium hydroxide. The second step can be referred to as the solvent-solvent extraction method. When two aqueous solutions are mixed, a Gd-carboxylate complex (GdR_3) is formed and precipitated immediately. These reactions produce water as a by-product, which can compromise the scintillation solution's performance. Although attempts are made to remove the water from samples as much as possible, a small portion of the water may still exist in the Gd-loaded LS [15]. The water impurities can scatter light and absorb certain wavelengths, reducing scintillation efficiency and the accuracy of neutrino interaction measurements. In addition, water can cause quenching effects and alter the chemical stability of the solution. Water is characterized by distinct vibrational modes that manifest as characteristic absorption peaks in the IR spectrum, including O-H stretching vibrations generally appearing around 3200–3600 cm^{-1} and H-O-H bending vibrations occur-

[2]The samples used in this study were prepared following the sample synthesizing methods mentioned in the RENO Technical Design Report (TDR) [13] utilizing the same materials.

ring around 1600 cm^{-1}. Identifying water from these distinct IR absorption peaks is essential for maintaining the purity and effectiveness of the scintillation medium, and thereby ensuring reliable experimental results.

Additionally, our analysis of three impurity compounds (IMP1, IMP2, and IMP3) provided further insights into their spectral characteristics. IMP1 ($C_{29}H_{20}N_2O_4$) exhibited strong absorption bands around 1730, 1800, and 1940 cm^{-1} for carbonyl (C=O) groups, and a significant absorption band near 1570 cm^{-1} for amide (C-N) groups. IMP2 ($C_{33}H_{38}ClNOS$) featured sulfoxide (S=O) and aryl chloride (Ar-Cl) groups, with absorption peaks at 1090 and 1140 cm^{-1}, respectively. IMP3 ($C_{34}H_{36}N_2O_4$) contained azo (N=N) and ether (C-O-C) groups, with characteristic peaks at 1550, 1180, and 1330 cm^{-1}. These detailed IR spectra and the analysis of these impurity compounds enabled us to confirm the absence of these impurities in the LAB (+ PPO + bis-MSB) sample.

The results of this study demonstrate that IR spectroscopy is a reliable method for identifying the existence of a quencher in scintillation solutions. In Fourier Transform Infrared (FTIR) measurement, the impact of water and acetone, such as ligand exchange in metal-loaded LAB, was significant at a concentration of approximately 4.5% in 100 ml, with no notable effect observed at concentrations of 0.9% or 9900 ppm. Furthermore, these results can be utilized to improve the reliability and precision of neutrino measurements.

Consequently, the IR spectrum and spectral analysis of the scintillation solutions have sufficient potential to enable understanding the optical properties and efficiency of neutrino detectors. This is because they can provide a complementary method to detect and identify impurities that are difficult to discern with only the UV/VIS spectrum. In particular, complex impurities in which nitrogen or oxygen replaces carbon can easily be identified by their unique absorption peaks in the IR spectrum.

The structure of this paper is as follows. Section 2 introduces the unique absorption frequencies corresponding to vibrational transitions among various atoms. Section 3 describes the preparation and measurement methods of the experimental samples prepared for this study as well as presents the spectra of synthetic solutions made from these materials and their analysis. Section 4 briefly discusses the sources of impurities and the IR spectrum results of the solvents and solutes of these liquid scintillation solutions. Section 5 describes the theoretical spectrum. Further, Section 6 discusses the spectra of synthetic solutions made from these materials and their analysis. Finally, Section 7 briefly summarizes and discusses the research findings, concluding the paper.

2. Comprehensive vibrational transition frequencies for various chemical bonds

Figure 2 shows the comprehensive vibrational transition frequencies for various chemical bonds found in experimental analysis. It includes the ranges for single, double, and/or triple bonds of C-C, C-O, C-N, N-O, and various other atom pairs as well as typical vibrational transitions for C-H, O-H, and N-H bonds in organic molecules. The colored bands highlight these important vibrational modes. From Fig. 2, it is easy to identify which specific bonds appear within certain frequency ranges. Notably, the region between 1800 and 2000 cm^{-1} has fewer bands due to the absence of triple bonds and specific double-bond transitions in typical organic molecules.

For more detailed information on IR spectroscopy and the IR spectra of various atomic bonds, readers are requested to refer to Chapter 2 and Table 2.3 of Ref. [16].

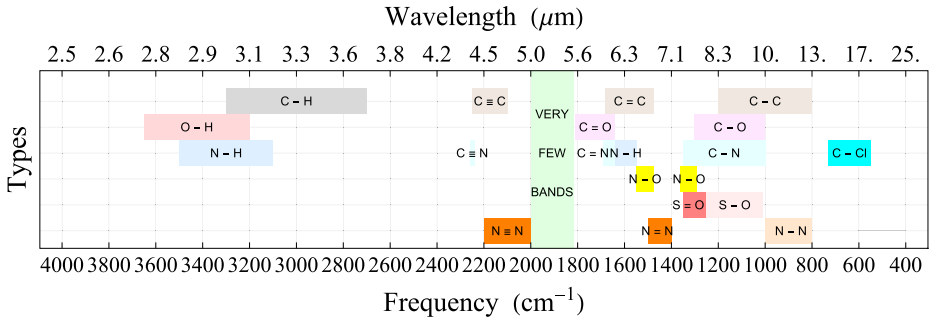

Fig. 2. Comprehensive vibrational transition frequencies for various chemical bonds encountered in experimental analysis. Colored bands indicate the spectral range of each vibrational frequency, highlighting the important vibrational modes. Notably, the region between 1800 and 2000 cm^{-1} exhibits fewer bands, primarily due to the general absence of triple bonds and specific double-bond transitions in typical organic molecules, which do not commonly fall within this frequency range. In addition, the ranges of frequency bands introduced here may be reduced or increased depending on the actual situation.

3. Experimental samples and IR measurements

In this study, LAB provided by Isu Chemical [17] was used as the solvent, while PPO and bis-MSB, purchased from Sigma-Aldrich, as the first scintillation fluor and secondary wavelength shifter fluor [18,19], were selected as solutes to synthesize the scintillation solutions. PPO and bis-MSB were mixed at 3 g/l and 30 mg/l, respectively, and LAB was used as received from the manufacturer without further purification using a gravity column adsorption technique with alumina (Al_2O_3) powder. The masses of the fluors PPO and bis-MSB were measured using a microbalance, and then they were dissolved in 1 l of LAB to prepare the standard scintillation solutions. From these solutions, 300-μl samples were prepared. To prevent a saturation response in the fluorescence spectrometer, the samples were further diluted by 300 times, with the concentrations and volume adjusted to PPO $\sim$ 0.01 g/l, bis-MSB 0.1 mg/l and 200 ml, respectively, and the final samples for the experiment were prepared. A volume of 5 ml of acetone was added dropwise to 100 ml of the diluted LAB + PPO sample using a pipette. The resulting solution was then stirred using a magnetic stirrer. The FTIR of the solution was immediately measured after stirring. The LAB + PPO + bis-MSB samples were mixed and measured in the same way as the LAB + PPO + acetone impurity samples, with the exception that water was added to the LAB + PPO + bis-MSB samples using a magnetic stirrer and commercial ultrasonic stirrer.

The descriptions of the IR experimental setup and method are as follows: The IR spectrum of the samples was measured in a single attenuated total reflectance (ATR) mode, with the signal collected after only one reflection. Liquid samples were measured by dropping a droplet onto a zinc selenide (ZnSe) single-crystal incident window. Powder samples were ground into a fine powder using a pestle and mortar, gathered on the ZnSe single-crystal window, and then pressed using a small rotary press for measurement. A schematic of the measurement methods according to the sample type is shown in Fig. 3.

In the following subsections, brief IR measurement results of the solvent LAB and the two solutes PPO and bis-MSB are mentioned, and the results of the final solution used are discussed (see Ref. [12] for the detailed IR results of these materials).

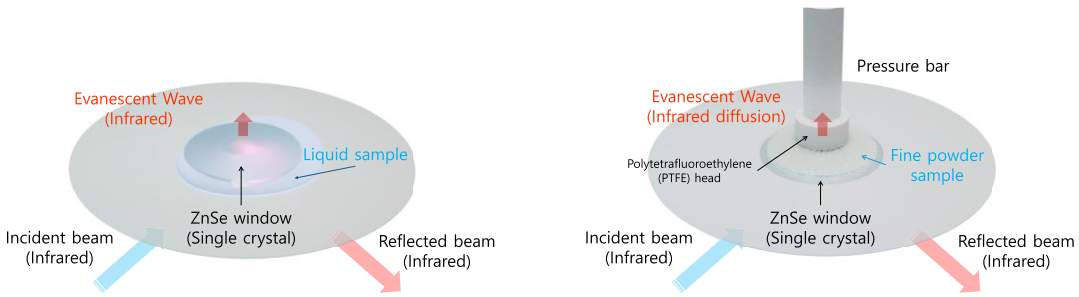

Fig. 3. Schematic of measuring liquid (left) and powder samples (right) on an FTIR spectrometer equipped with an ATR module. The baseline data for the IR measurement instrument were acquired in a laboratory environment where the atmosphere was in equilibrium. Baseline readjustments were conducted in real time following the acquisition of each IR measurement. The settings of the IR measurement instrument were configured in accordance with the manufacturer's recommendations. In particular, the default resolution was set to 2 cm^{-1}, with the exception of instances where 0.5 and 1 cm^{-1} resolutions were required.

3.1. *LAB*

A strong absorption peak corresponding to the C-H stretching mode of the benzene ring appeared near 3000 cm^{-1}, and the C-H stretching modes of the alkyl chains also appeared in the 2850–2950 cm^{-1} range. These latter modes generally correspond to sp_3 hybridization and have a slightly smaller wavenumber compared to the benzene ring stretching modes. Similarly, the bending modes of the benzene ring C-H and alkyl chains appear around 1600 and 1500 cm^{-1}, respectively, whereas slower C-H bending modes of the chains and out-of-plane bending modes of the benzene ring appear in the 700–800 cm^{-1} range.

3.2. *PPO powder*

A stretching peak of the C-H bond of the benzene ring was visible near 3100 cm^{-1}, and a little to the left a smaller stretching peak of the C-H bond of the oxazole ring at a slightly higher wavenumber was seen. Near 1500 cm^{-1}, bending modes of the PPO molecule existed (including the C-N stretching mode), and lower-wavenumber bending vibration modes were observed particularly around 700 cm^{-1}. Additionally, peaks involving three C-O stretchings were observed around 1100, 1200, and 1300 cm^{-1}.

3.3. *bis-MSB powder*

Three peaks could be seen near 3000 cm^{-1}, which were the C-H stretching peaks of the benzene rings. In the order of greatest magnitude, these peaks are associated with the sp_2 C-H stretching mode of the central benzene ring and the asymmetric and symmetric stretching modes of the methyl groups (-CH3) attached on either side. The large peak near 1500 cm^{-1} is indicative of the rocking bending mode of the central benzene ring's C-H bonds, and the peaks below 1000 cm^{-1} correspond to the lower-frequency twisting and bending modes of bis-MSB.

3.4. *Scintillation solution (LAB + PPO + bis-MSB)*

Given that the concentrations of PPO and bis-MSB in the solution are lower than that of LAB, their distinct absorption peaks are barely noticeable. Thus, any slight increase or decrease in LAB's transmittance can be easily detected. This phenomenon was confirmed by experimental

results. The increase and decrease (from low- to high-frequency regions) are similar to the sum of the two solute effects (less than 1% each), ultimately (based on the transmittance of LAB) affording a transmittance increase of up to 2% around 3500 cm^{-1}. Interestingly, only around 2900 cm^{-1}, the transmittance showed a temporary decrease of $\sim$ 5% based on a trend line that gradually increased to 2%. This is presumably the result of complex interactions between PPO and bis-MSB within LAB.

4. Sources of impurities

Understanding the sources of impurities in scintillation solutions is essential for maintaining the high performance and accuracy of neutrino detectors. Impurities can arise from various stages of material production and experimental operation. We classify these sources into four main categories, which are described in the following subsections.

4.1. *Raw chemical production*

During the production of raw chemicals, impurities can be introduced at the initial stage of manufacturing. These impurities may include residual solvents, by-products from chemical reactions, or contaminants from raw material extraction and refinement processes. For instance, trace metals or organic contaminants can originate from the initial raw materials used. The unknown impurities mentioned by the JUNO Collaboration research group likely fall into this category [14].

4.2. *Synthesis to LS*

The synthesis of fine chemicals from raw materials can introduce additional impurities. These impurities can originate from the synthesis environment, such as contamination from reaction vessels or residual solvents. Additionally, chemical processes can generate by-products, particularly when dealing with complex reactions. For example, during metal ligand processing, by-products from acid–base reactions may be introduced into the final product. Water, produced as a by-product during neutralization reactions, falls into this category.

4.3. *Experimental operation*

During the operation of experiments, impurities can be introduced by various means. Contamination of the scintillation solution can occur because of several factors, including nitrogen purging of the solution, trial runs that bury visible light or radioactive sources in the solution, exposure of the solution to high-humidity environments, and routine maintenance. For example, the use of gases for purging can introduce trace contaminants if the gases are not of high purity. Similarly, equipment used in maintenance can carry residues that may contaminate the solution. Human error, such as improper handling and lack of training or inexperience, can also introduce impurities such as acetone and other contaminants during measurement.

4.4. *Natural degradation*

Over time, scintillation solutions can undergo natural degradation, leading to the formation of impurities. This can occur via processes such as oxidation, hydrolysis, or photodegradation. For instance, prolonged exposure to light or elevated temperatures can cause the breakdown of chemical components, resulting in degradation products that act as impurities. The unknown impurities mentioned by the JUNO Collaboration could also belong to this category.

By understanding and identifying the aforementioned sources of impurities, their presence in liquid scintillation solutions can be better controlled and mitigated. In the next section, we discuss these impurities in more detail, focusing on their identification and effect on the performance of scintillation solutions.

5. Theoretical spectrum calculations

This section outlines the method, basis set, and commands used in the G16 software suite for IR spectrum calculations. To accurately model vibrational transitions and predict IR spectra of impurities in our scintillation solutions, we employed the PBE1PBE (PBE0) functional, a hybrid approach in Density Functional Theory (DFT). PBE0 combines the Perdew–Burke–Ernzerhof (PBE) exchange-correlation functional with 25% Hartree–Fock exchange energy, offering improved accuracy over pure DFT methods. This hybrid approach balances computational efficiency and accuracy, making it suitable for systems with a moderate number of atoms. PBE0 excels in structural optimization, vibrational frequency calculations, thermochemical predictions, and computing spectroscopic properties like IR spectra, making it ideal for studying transition metal compounds and organic molecules where accurate electronic interactions are crucial.

We selected the 6-311+G(2df,p) basis set for its detailed representation of molecular orbitals and electronic interactions. This basis set uses six Gaussian functions for core electrons, providing a robust description of inner-shell electrons. The "311" component describes valence electrons with three different-sized basis functions, allowing for flexible and accurate bonding representation. The "G" indicates the addition of diffuse functions, essential for modeling weakly bound electron interactions. The "(2df,p)" specifies polarization functions, enhancing the basis set's ability to model electron cloud flexibility during chemical bonding. This configuration is particularly effective for organic molecules with key functional groups such as carbonyl (C=O), amide (C-N), sulfoxide (S=O), aryl chloride (Ar-Cl), azo (N=N), and ether (C-O-C). These groups influence the optical properties of scintillation solutions and are detectable through unique vibrational modes in the IR spectrum.

Geometry optimizations and frequency calculations for the impurity compounds IMP1, IMP2, and IMP3 were conducted in G16 using the OPT and FREQ commands. We applied standard convergence criteria, setting an energy threshold of approximately 10^{-5} Hartree. All calculations assumed a neutral charge and singlet spin state for the impurity compounds.

The theoretical IR spectra generated from these calculations identify characteristic absorption bands that can be used to detect impurities. These spectra serve as benchmarks for comparison with experimental IR data to confirm the absence of significant impurity peaks in our LAB (+ PPO + bis-MSB) samples, ensuring the purity and high performance of the scintillation solutions used in neutrino detection experiments.

6. Identification of impurities in scintillation solutions

In this section, we discuss how to identify impurities if they are present in the scintillation solution. As practical examples, the cases of acetone and water are introduced in turn, and the cases of the three types of impurity compounds mentioned by the JUNO Collaboration are discussed at the end.

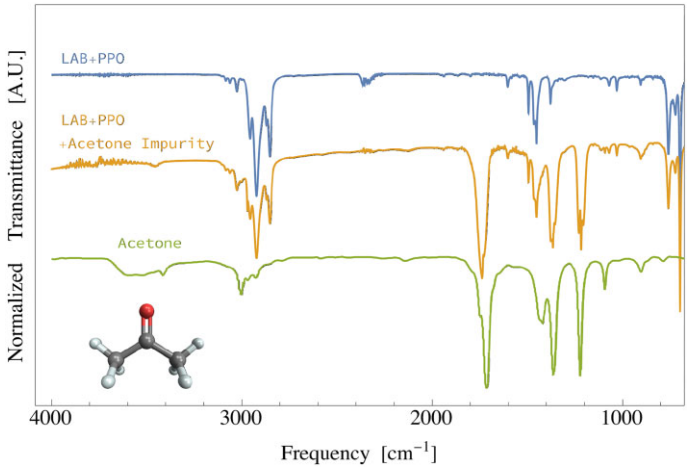

Fig. 4. Comparison of the IR spectra of (LAB + PPO) solutions with and without acetone impurities. The blue line at the top represents the spectrum of (LAB + PPO) without impurities, the orange line in the middle shows the spectrum for acetone included as an impurity, and the green line at the bottom displays the spectrum of acetone alone. The dips at 1200, 1400, and 1700 cm^{-1} in the middle spectrum indicate the effect of acetone impurities, confirmed by the corresponding dips in the acetone-only spectrum.

6.1. *Acetone impurity*

Cleaning solvents are widely used to clean scientific equipment due to their rapid evaporation and residue-free properties. However, residual cleaning liquids can contaminate samples before complete evaporation, so caution is advised. Figure 4 shows the IR spectrum (middle orange line) of a LAB solution mixed with PPO and containing acetone as an impurity. Additionally, the spectrum of the solution (LAB + PPO) without impurities (blue line) is shown at the top, and the one of acetone only (green line) is shown at the bottom for comparison. Comparing the top and middle lines indicates that the deep lines at 1200, 1400, and 1700 cm^{-1} are created by impurities. The bottom line (IR spectrum of acetone alone) confirms that the three dips due to this impurity are caused by acetone. In particular, the frequency around 1750 cm^{-1} corresponds to the stretching mode of carbon and oxygen double bonds, and each of 1200 and 1360 cm^{-1} corresponds to the bending mode between C-H and C-C.

6.2. *Water impurity*

In the preparation of Gd-loaded LAB-based LS [15] used in neutrino oscillation experiments, the formation of water through chemical reactions is an essential consideration. The process can be represented by the following chemical equations:

$$\mathrm{RCOOH} + \mathrm{NH_3 \cdot H_2O} \rightarrow \mathrm{RCOONH_4} + \mathrm{H_2O} \tag{1}$$

$$\mathrm{GdCl_{3\,(aq)}} + 3\mathrm{RCOOH_{4\,(aq)}} \rightarrow \mathrm{Gd(RCOO)_3} + 3\mathrm{NH_4Cl} \tag{2}$$

where RCOOH represents a carboxylic acid, and $\mathrm{Gd(RCOO)_3}$ is the gadolinium complex formed. The by-product, water, can affect the performance of the scintillation solution used in neutrino detectors. It is significant owing to several reasons: First, as an impurity in the scintillation medium, water can compromise the optical clarity of the solution. Even minor amounts of water can scatter light and absorb certain wavelengths, which reduces the scintillation efficiency. This decline directly affects the detector's capability to measure neutrino interactions accurately. Second, water molecules can interact with the excited states of the scin-

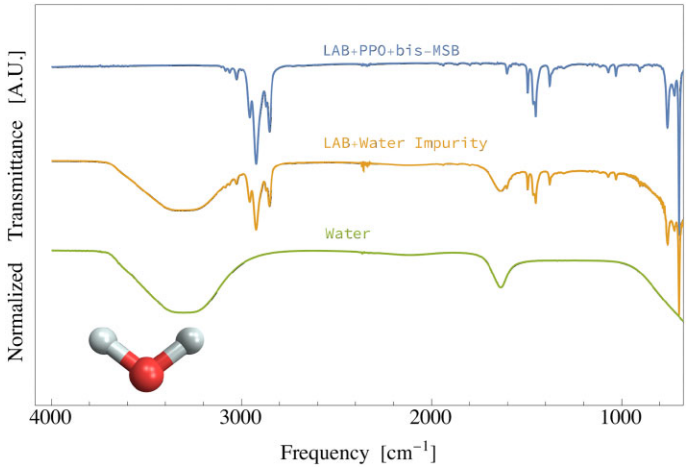

Fig. 5. Same as Fig. 4, but the solution is LAB and the impurities are water molecules. The dips around 3300 and 1600 cm^{-1} in the middle spectrum indicate the effect of water impurities, confirmed by the corresponding dips in the water-only spectrum.

tillator molecules or with the products of neutrino interactions. They can cause nonradiative de-excitations, a phenomenon known as quenching, which reduces the light yield of the scintillator. Third, the presence of water can alter the chemical stability of the scintillation solution. It may cause the hydrolysis of some components, particularly in the presence of metal ions such as Gd, potentially altering the chemical composition over time.

A water molecule is characterized by distinct vibrational modes that manifest as characteristic absorption peaks in the IR spectrum. These include the O-H stretching vibrations, which generally appear around 3200–3600 cm^{-1} and represent the most intense peak due to hydrogen bonding between water molecules.

The H-O-H bending vibration occurs around 1600 cm^{-1}, attributed to the bending motion of hydrogen atoms relative to the oxygen atom. Additionally, vibrational modes found roughly around 720 cm^{-1} are related to the restricted rotational motion of water molecules within the hydrogen-bonded network.

At the top of Fig. 5, a blue line indicates the case of LAB containing no impurities, and at the bottom, a light-green line indicates the case of water only. Comparing the top and middle lines, we notice two new absorption peaks around 3300 and 1600 cm^{-1} due to impurities. Comparing the middle and bottom lines, we deduce that these absorption peaks are caused by water molecules (see also Fig. 7: the fourth and fifth line plots from the top). Identifying and quantifying these two peaks in the IR spectrum of a scintillation solution can provide essential data on the presence and concentration of water.

6.3. *Impurity compounds (IMP1, IMP2, IMP3)*

Our analysis focused on the characteristics and molecular structures of impurity compounds as specified in prior research from the JUNO Collaboration, particularly focusing on their molecular bonds and absorption properties [14]. The impurity compounds, classified as impurity compounds I, II, and III (IMP1, IMP2, and IMP3), are crucial because of their distinctive UV/VIS absorption peaks, which significantly affect the performance of neutrino oscillation experiments. Their molecular structures are shown in order from left to right in Fig. 6. IMP1, identified with the molecular structure $C_{29}H_{20}N_2O_4$, features prominent bonds such as C=O

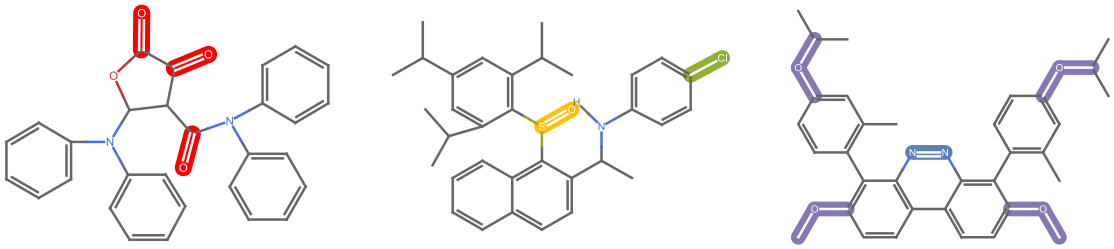

Fig. 6. Molecular structures of IMP1, IMP2, and IMP3, highlighting their key functional groups in different colors. IMP1 contains benzene rings, carbonyl groups, and amide groups, notably with three C=O absorptions around 1730, 1800, and 1940 cm^{-1}, and C-N absorptions near 1610 cm^{-1}. IMP2 features benzene rings, a sulfoxide group, a thioether group, and an aryl chloride, with significant absorptions in the ranges of 1030–1090 cm^{-1} for S=O, 700–1000 cm^{-1} for C-S-C, and 1140 cm^{-1} for Ar-Cl. IMP3 includes benzene rings, an azo group, and ether linkages, with prominent absorptions around 1650 cm^{-1} for N=N and 1180 and 1330 cm^{-1} for C-O-C. Note that the frequency for each functional group was calculated using Gaussian16 by the PEB0 DFT method based on the 6-311+G(2df,p) basis.

and C-N, which are also known for their absorption around 440.89 nm in the UV/VIS spectrum. IMP2, with the molecular formula $C_{33}H_{38}ClNOS$, includes critical bonds like S=O and C-Cl, absorbing light at about 413.51 nm. Finally, IMP3, which has the molecular formula $C_{34}H_{36}N_2O_4$, displays significant N=N and C-O-CH3 bonds, with an expected absorption peak at 419.88 nm.

These specific bonds in each molecule are crucial in the IR spectrum because they correspond to unique vibrational modes that can easily be identified using IR spectroscopy. The distinctive IR frequencies associated with some functional groups help in accurately identifying the presence of these impurities within the scintillator solutions. However, because these molecular structures could not be directly synthesized in this study, the IR spectra of the impurities could not be confirmed by experiments. Instead, their IR spectra were calculated theoretically using G16 software [11]. The PBE0 hybrid DFT [20,21][3] and 6311+g(2df,p) basis [22], previously used by the JUNO Collaboration for UV/VIS studies of impurities, were consistently used for our IR analysis.

Figure 7 shows the calculation results of the IR spectrum of each impurity compound's molecule in the form of a line plot. The results for IMP1, IMP2, and IMP3 are shown in order from sixth to eighth, with the main absorption lines shown as lines for ease of comparison. Note again that the width of the absorption lines is determined by a specific absorption rate. This criterion was set to obtain clearer major specific absorption lines for each molecule.

6.3.1. *IMP1.* The molecular structure of IMP1 features several prominent functional groups. The aromatic rings in the molecule are expected to produce C-H stretching vibrations. These vibrations typically occur in the range of 3000–3100 cm^{-1}. However, our calculations

[3]To compare the accuracy of our DFT calculations, we used both PBE0 [20,21] and B3LYP [23–25] functionals. At higher frequencies (around 3000 cm^{-1}), PBE0 results were $30 \sim 40$ cm^{-1} higher than those of B3LYP, due to the stronger exchange interaction from the 25% Hartree–Fock exchange in PBE0. In the lower-frequency region, both functionals produced similar results, as weak bending vibrations are less sensitive to exchange interactions and the Generalized Gradient Approximation (GGA) components dominate.

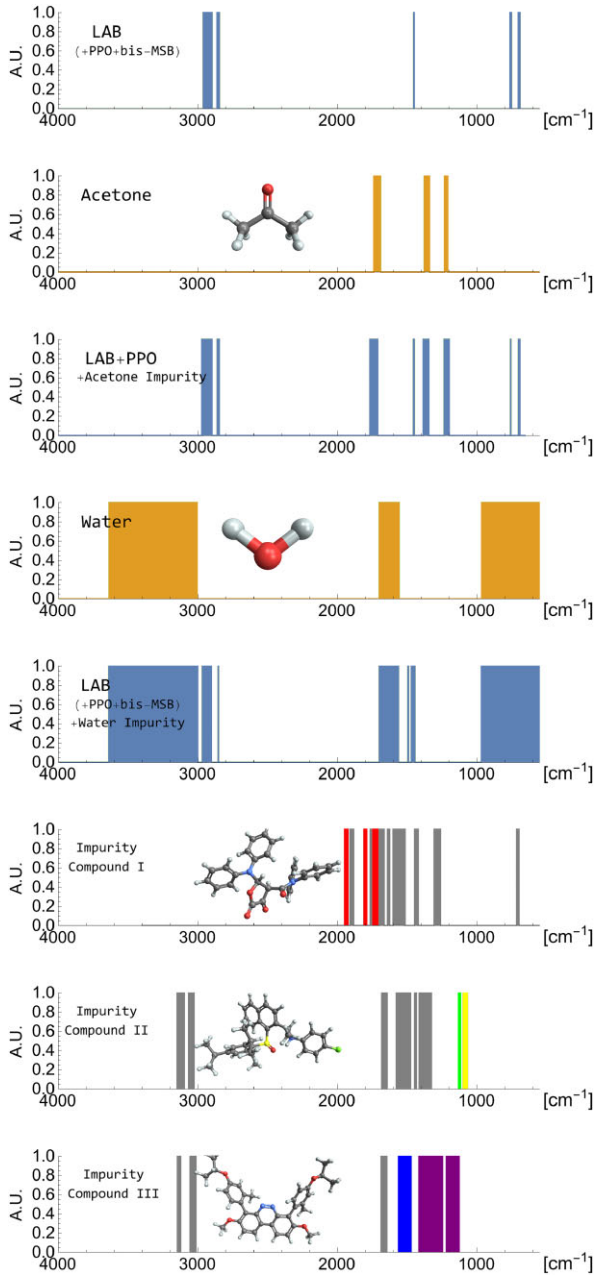

Fig. 7. IR spectra of LAB (+ PPO + bis-MSB) solution and various impurities. The width of each band does not represent the absolute intensity of the absorption line. Instead, it only indicates the peak location and the relative absorption intensity at that peak. The top spectrum (blue line) represents LAB (+ PPO + bis-MSB) without impurities. The second spectrum illustrates the IR spectrum of pure acetone. The third spectrum shows LAB (+ PPO) mixed with acetone impurity, displaying distinct absorption peaks at 1200, 1360, and 1700 cm^{-1}. The fourth spectrum shows the IR spectrum of pure water. The fifth spectrum presents LAB (+ PPO + bis-MSB) mixed with water impurity, with characteristic absorption peaks at 3300 and 1600 cm^{-1}. The bottom three spectra are the calculated IR spectra of impurity compounds I, II, and III (IMP1, IMP2, and IMP3). IMP1 shows strong absorption bands around 1730, 1800, and 1940 cm^{-1} for carbonyl groups (C=O), highlighted in red, and around 1570 cm^{-1} for amide groups (C-N). IMP2 features sulfoxide (S=O) and aryl chloride (Ar-Cl) absorption lines at 1090 and 1140 cm^{-1}, highlighted in yellow and green, respectively. IMP3 displays N=N and C-O-C stretching vibrations around 1550, 1180, and 1330 cm^{-1}, highlighted in blue and purple, respectively. These spectra confirm that the LAB (+ PPO + bis-MSB) sample we manufactured is free of the impurities tested, ensuring high performance and accuracy in neutrino detection.

show that in IMP1, they appear around 3200 cm^{-1}. Although these C-H stretching modes near 3200 cm^{-1} are present in the spectrum, they are not marked on the line plot owing to their weaker intensity compared to other absorption lines. Additionally, various bending modes typically appear below 1700 cm^{-1}. The three carbonyl groups (C=O) present in the structure (starting at 12 o'clock in the order of clockwise rotation in Fig. 6) correspond to strong absorption bands around 1730, 1800, and 1940 cm^{-1}. These three absorption lines, representing this impurity, are highlighted in red in Fig. 7. Furthermore, the amide groups exhibit C-N bond vibrations, which, although often mixed with other vibrational modes, are significantly associated with one very strong absorption band near 1570 cm^{-1}.

6.3.2. *IMP2.* The molecular structure of IMP2 includes several key functional groups. The N-H bond is expected to exhibit stretching vibrations around 3600 cm^{-1}, but its intensity is weaker than those of other absorption lines; therefore, it is not displayed in this line plot. Unlike the case of the benzene ring of IMP1, the benzene ring of IMP2 has sufficiently strong absorption intensity and exhibits various C-H stretching vibrations around 3200 cm^{-1}. The C=C stretching vibrations appear around 1580 and 1680 cm^{-1}. The sulfoxide group (S=O) is expected to show a strong S=O stretching absorption around 1090 cm^{-1}. Further, the thioether group (C-S-C) in the molecule typically exhibits stretching vibrations around 700–1000 cm^{-1}. The aryl chloride (Ar-Cl), where a chlorine atom is directly bonded to an aromatic ring, shows a stretching vibration around 1140 cm^{-1}. In Fig. 7, Ar-Cl and S=O were selected as absorption lines representing this impurity and highlighted with green and yellow lines, respectively.

6.3.3. *IMP3.* IMP3 has a crab-shaped molecular structure, with an N=N bond in the middle of the three benzene rings and four C-O-C bonds in the crab-like branches. The benzene rings in the structure show C-H stretching vibrations above 3000 cm^{-1} and various bending modes appear below 1650 cm^{-1}. The azo group (N=N) is expected to display stretching vibrations around 1550 cm^{-1}. The ether group (C-O-C) often shows the C-O stretching vibrations around 1180 and 1330 cm^{-1}. These N=N and C-O-C bonds were selected as bonds representing this molecule; these are shown as blue and purple lines, respectively, in Fig. 7. Note that the purple band includes not only N=N vibrations but also other banding modes, and the line width is relatively wider owing to the four types of branches.

Consequently, the presence of these impurity compounds could be expected if distinct peaks corresponding to some of the following groups are observed: carbonyl (C=O), amide (C-N), sulfoxide (S=O), azo (N=N), and aryl chloride (Ar-Cl).[4] Conversely, if their distinctive absorption lines are not found in the solution, it can be concluded that these impurities are not present. In Fig. 7, these impurities evidently do not exist in the LAB (+ PPO + bis-MSB) sample that we fabricated. This detailed spectroscopic analysis is imperative for ensuring the high performance of neutrino detectors, as the presence of such impurities can lead to significant losses in light transmission, thereby affecting the detector's efficiency and the accuracy of neutrino detection.

[4]Fitting all the absorption lines that are omitted or not discussed in this study may not be practical because of their weak absorption and diffuseness. Therefore, while the presence of the main absorption lines is necessary to indicate the presence of certain impurities, it alone is not sufficient to confirm their presence. This is because different types of molecular structures containing these bonds and having the same chemical formula are possible.

7. Conclusion and implication

In this study, we focused on the identification and analysis of impurities in LAB-based scintillation solutions using IR spectroscopy. Our approach provides a detailed spectral analysis that complements previous research, which primarily utilized UV/VIS spectra to investigate electronic structures and transitions.

Previous studies have shown that LAB-based scintillation solutions, commonly used in neutrino oscillation experiments, exhibit unique IR absorption characteristics. The IR absorption peaks of LAB are largely insensitive to the alkyl chain length, although the intensity decreases with longer chains. Additionally, PPO and bis-MSB have distinct IR spectra in both powder and solution forms, indicating interactions between these solutes and LAB. These foundational studies provide a critical understanding of the vibrational modes of the base components.

In our current research, we extended this analysis to detect specific impurities in LAB solutions, namely, acetone and water impurities, and three impurity compounds (IMP1, IMP2, and IMP3) identified by the JUNO Collaboration.

Acetone is used extensively in the cleaning and preparation of various types of scientific equipment and optical components because it evaporates quickly and leaves no residue. This makes it ideal for preparing items that must be completely free of impurities, such as lenses and other delicate instruments used in optics. However, residual acetone before complete evaporation may mix with the sample being observed, leaving unnecessary traces. The presence of acetone, labeled as acetone impurity, in LAB solutions was identified by distinct absorption peaks at 1200, 1360, and 1700 cm^{-1}. These peaks correspond to the C-H and C-C bending modes and the C=O stretching mode, respectively. Water, labeled as water impurity, can be introduced during the preparation of Gd-loaded LAB. It significantly affects scintillation efficiency by scattering light and causing quenching effects. The IR spectrum of water showed characteristic O-H stretching vibrations around 3200–3600 cm^{-1} and H-O-H bending vibrations around 1600 cm^{-1}. The presence of these peaks in LAB solutions indicates water contamination.

The analysis of impurity compounds provided further insights into the spectral characteristics of potential contaminants. The first impurity compound, IMP1, with the molecular formula $C_{29}H_{20}N_2O_4$, showed strong absorption bands around 1730, 1800, and 1940 cm^{-1} for carbonyl (C=O) groups, and a significant absorption band near 1570 cm^{-1} for amide (C-N) groups. These peaks are critical for identifying IMP1 in LAB solutions. The second impurity compound, IMP2, with the molecular formula $C_{33}H_{38}ClNOS$, includes key functional groups such as sulfoxide (S=O) and aryl chloride (Ar-Cl). The S=O stretching vibration appears around 1090 cm^{-1}, whereas the Ar-Cl stretching vibration is observed at 1140 cm^{-1}. These distinct peaks facilitate the detection of IMP2. The third impurity compound, IMP3, with the molecular formula $C_{34}H_{36}N_2O_4$, features azo (N=N) and ether (C-O-C) groups. The N=N stretching vibration appears around 1550 cm^{-1}, and the C-O stretching vibrations are observed at 1180 and 1330 cm^{-1}. These characteristic peaks are essential for identifying IMP3.

For a specific ZnSe crystal size and IR spectrum obtained in single reflection mode, the water or acetone effect was significant at concentrations to about 4.5%, and undetectable below this level. These detailed IR spectra and the analysis of these impurity compounds enabled us to confirm the absence of these impurities in the LAB (+ PPO + bis-MSB) sample within the IR measurement limit. Molecular spectroscopic techniques, including complementary FTIR

and UV/VIS spectroscopy, can provide the assurance required that the levels of impurities in LS are within acceptable limits. This assurance is crucial for maintaining the high performance and accuracy of neutrino detectors, as the presence of impurities can cause significant losses in light transmission and affect the detector's efficiency.

This study underscores the effectiveness of IR spectroscopy as a powerful analytical tool for detecting and identifying impurities in scintillation solutions. By leveraging the unique spectral signatures of various functional groups, the purity of the scintillation medium can be ensured, thereby enhancing the reliability and precision of neutrino detection experiments. The computational utility of DFT is being demonstrated for phenomena involving the presence of exotic molecules and collective motion in condensed matter physics and nuclear astrophysics. Accordingly, G16 was chosen as a computational tool for quantum chemistry of highly symmetric liquid states. Using G16, we have been able to model and analyze the electronic structure and properties of molecules in the liquid state, providing insights that would be difficult to obtain by experimental means alone. To date, there have been no experiments or research and development studies using IR spectroscopy to identify impurities. Therefore, the proposed method has sufficient potential for quality control applications during LS synthesis. Our findings provide a robust framework for quality assurance in the preparation of scintillation solutions, contributing to the overall success of neutrino oscillation research.

Funding

This research was supported by a grant from the National Research Foundation of Korea (Grant No. NRF-2020R1A2C3006177, Grant No. NRF-2021R1A6A1A03043957, NRF-2022R1A5A1030700, NRF-2022R1A2C1006069, and 2018R1D1A1B07051126).

References

[1] J. S. Park et al., Nucl. Instrum. Methods Phys. Res. A **707**, 45 (2013).
[2] F. P. An et al., Nucl. Instrum. Meth. A **685**, 78 (2012).
[3] S. Andringa et al., Adv. High Energy Phys. **2016**, 6194250 (2016).
[4] V. Fischer, [SNO+][arXiv:1809.05986 [physics.ins-det], 17 Sep. 2018], https://doi.org/10.48550/arXiv.1809.05986. (accessed 2024-10-16).
[5] C. Aberle, C. Buck, B. Gramlich, F. X. Hartmann, M. Lindner, S. Schönert, U. Schwan, S. Wagner, and H. Watanabe, J. Instrum. **7**, P06008 (2012) [arXiv:1112.5941 [physics.ins-det], 27 Dec. 2011 (accessed 2024-10-16).
[6] F. An et al., J. Phys. G **43**, 030401 (2016) [arXiv:1507.05613 [physics.ins-det], 18 Oct. 2015] (accessed 2024-10-16).
[7] S. Ajimura et al., Nucl. Instrum. Methods Phys. Res. A **1014**, 165742 (2021).
[8] T. Maruyama, PoS **NuFact2021**, 159 (2022).
[9] M. C. Chen, AIP Conf. Proc. **944**, 25 (2007).
[10] J. Y. Choi, J. B. Park, and K. K. Joo, New Phys.: Sae Mulli **73**, 866 (2023) (in Korean).
[11] M. J. Frisch et al., Gaussian 16 (Gaussian, Inc., Wallingford, CT, 2016).
[12] J. Y. Choi, J. B. Park, and K. K. Joo, New Phys.: Sae Mulli **74**, 746 (2024) (in Korean).
[13] RENO Collaboration, J. K. Ahn, et al., [arXiv:1003.1391 [hep-ex], 6 March 2010], https://doi.org/10.48550/arXiv.1003.1391(accessed 2024-10-16).
[14] D. Cao et al., Nucl. Instrum. Methods Phys. Res. A **927**, 230 (2019).
[15] Y. Ding, Z. Zhang, J. Liu, Z. Wang, P. Zhou, and Y. Zhao, Nucl. Instrum. Methods Phys. Res. A **584**, 238 (2008).
[16] D. L. Pavia, G. M. Lampman, G. S. Kriz, and J. A. Vyvyan, Introduction to Spectroscopy (Cengage Learning, Boston, MA, 2015), 5th ed.

[17] ISU Chemical, "Petrochemical Products: LAB", CAS RN: 67774-74-7 (ISU Chemical, Seoul). (Available at: https://www.isuchemical.com/eng/business/getBiz1004Html.do, date last accessed June 30, 2024).
[18] Sigma-Aldrich, "2,5-Diphenyloxazole", CAS RN: 92-71-7 (Sigma-Aldrich, Darmstadt) . (Available at: https://www.sigmaaldrich.com/product/sigma/d4630, date last accessed June 30, 2024).
[19] Sigma-Aldrich, "1,4-Bis(2-methylstyryl)benzene", CAS RN: 13280-61-0 (Sigma-Aldrich, Darmstadt). (Available at: https://www.sigmaaldrich.com/product/sigma/15090, date last accessed June 30, 2024).
[20] J. P. Perdew, M. Ernzerhof, and K. Burke, J. Chem. Phys. **105**, 9982 (1996).
[21] C. Adamo and V. Barone, J. Chem. Phys. **110**, 6158 (1999).
[22] R. Krishnan, J. S. Binkley, R. Seeger, and J. A. Pople, J. Chem. Phys. **72**, 650 (1980).
[23] A. D. Becke, J. Chem. Phys. **98**, 5648 (1993).
[24] A. D. Becke, Phys. Rev. A **38**, 3098 (1988).
[25] C. Lee, W. Yang, and R. G. Parr, Phys. Rev. B **37**, 785 (1988).